Chemical Engineering Journal 155 (2009) 94–100

Contents lists available at ScienceDirect

Chemical Engineering Journal

journal homepage: www.elsevier.com/locate/cej

Catalytic combustion of toluene over Mn, Fe and Co-exchanged clinoptilolite support

Zeynep Özçelik, Gülin S. Pozan Soylu*, İsmail Boz

Istanbul University, Faculty of Engineering, Chemical Engineering Department, Avcilar 34320, Istanbul, Turkey

ARTICLE INFO

Article history:
Received 9 March 2009
Received in revised form 25 June 2009
Accepted 1 July 2009

Keywords:
Catalytic oxidation
Toluene
Transition metals
Clinoptilolite
Acidity

ABSTRACT

Catalytic combustion of toluene over Fe, Co, and Mn transition metal oxides catalysts supported on clinoptilolite (CLT) has been investigated. The catalysts have been characterized by X-ray diffraction (XRD), scanning electron microscopy (SEM), temperature-programmed reduction and oxidation (TPR/TPO) and thermogravimetric analysis (TGA). 9.5MnO_2/NaCLT catalyst exhibited the catalytic activity, over which the toluene conversion reached to 93% at a temperature of 350 °C. The increase in activity was followed by increasing metal oxide content and gave a optimum at 9.5% MnO_2 loading. Addition of metal oxide into clinoptilolite support led to a measurable decrease in the onset of combustion and an increase in toluene conversion.

1. Introduction

Volatile organic compounds (VOCs) are important group of air pollutants. VOCs include any organic compound present in the atmosphere. Vehicle emissions, power generation and solvents emissions are considered to be the major sources of VOCs [1].

Several countries and organizations are now regulating the VOC levels of industrial emissions with the goal of improving air quality. Perhaps being stricter of all, California has been regulating the VOC content even in consumer products for several years now. Such VOC containing products are subject to Environmental Protection Agency (EPA) laws. For instance, Wood floor Varnish (finishes) would have a maximum allowable limit of 350 g/l.

Emission limits in Turkey (Law No. 2872) and Europe on the limitation of emissions of volatile organic compounds due to the use of organic solvents in certain activities and installations are set by Council Directive 1999/13/EC of 11 March 1999. Typically limit values are less than 50 mg C/N m^3 in waste gases [2].

Of course, the selection of removal technology depended on many parameters. However, the most common methods for VOC removal were thermal incineration and catalytic oxidation. From an economical point of view, catalytic oxidation of VOCs is an interesting technology due to the energy saving features and to the fact that the formation of by-products, such as dioxins and nitrogen oxides (NOx), can be minimized. Moreover, catalytic oxidation appears to be more efficient for the abatement of low concentrations of contaminant (<1000 ppm), which cannot be thermally combusted without additional fuel [3].

Noble metal catalysts are known to be very active in non-halogenated VOC removal. Supported Pt and Pd catalysts have been most widely studied for this purpose. In general, noble metal catalysts had a greater activity than other metal catalysts, but their manufacturing cost was high and can be easily deactivated by either sintering or poisoning by chlorine, sulfur or metals in the gas stream. For these reasons, there are strong interests to develop alternative efficient oxide based catalysts for VOC oxidation, especially utilizing natural abundant cheap resources. The advantages of developing catalysts based on transition metal oxides were associated with their lower cost, as well as the possibly higher thermal stability, resistance to humidity, increased specific surface area and greater resistance to common poisons [4–11]. Zeolites, i.e., clinoptilolite, have been claimed as promising supports to stabilize and provide high surface area support to transition metals [12].

The availability of zeolites with myriad of pore structures, composition and degree of hydrophobicity as well as the possibility to control the acidic properties have contributed to the increased usages of zeolites [13].

The scope of this work was to study the catalytic activity of the Gördes (Turkey) clinoptilolite impregnated with different transition metals' oxides (Fe, Co, Mn) in the catalytic combustion of toluene in air, and correlate these results with the physicochemical properties of clinoptilolite.

---

* Corresponding author. Tel.: +90 212 473 70 70x17665; fax: +90 212 591 1997.
E-mail addresses: gpozan@istanbul.edu.tr (G.S.P. Soylu), ismailb@istanbul.edu.tr (İ. Boz).

1385-8947/$ – see front matter © 2009 Elsevier B.V. All rights reserved.
doi:10.1016/j.cej.2009.07.013

Table 1
Metal oxide content, crystallite size, crystallinity of catalysts, T_{50}–T_{90} values, conversion to CO_2 at 350 °C and BET surface area.

Catalyst (metal oxide/zeolite)	Metal oxide content (wt%)	Crystallite size (nm)	Crystallinity (%)	BET surface area ($m^2\,g^{-1}$)	T_{50}–T_{90} (°C)	Conversion to CO_2 at 350 °C (%)
9.5Fe_2O_3/NaCLT	9.40 Fe_2O_3	41.23	88.23	21	–	16.90
5Fe_2O_3/NaCLT	4.87 Fe_2O_3	32.33	71.75	17	–	11.12
3Fe_2O_3/NaCLT	2.91 Fe_2O_3	20.23	64.56	13	–	2.67
9.5Co_3O_4/NaCLT	9.42 Co_3O_4	46.15	93.42	26	–	32.08
5Co_3O_4/NaCLT	4.79 Co_3O_4	37.05	83.30	21	–	14.96
3Co_3O_4/NaCLT	2.82 Co_3O_4	29.21	72.34	17	–	10.51
9.5MnO_2/NaCLT	9.43 MnO_2	64.70	94.64	32	302–348	93.02
5MnO_2/NaCLT	4.89 MnO_2	27.94	90.82	26	–	32.71
3MnO_2/NaCLT	2.97 MnO_2	17.69	73.28	22	–	20.51
9.5MnO_2/HZSM-5	9.46 MnO_2	24.84	92.65	154	–	24.78
MnO_2	–	–	–		328–439	64.05
NaCLT	–	–	–		492	14.09

2. Experimental

2.1. Characterization techniques

Clinoptilolite used in this study was obtained from the Gördes deposit in Aegean Sea region of Turkey. The clinoptilolite-rich mineral from Gördes was characterized by using X-ray diffraction (XRD), scanning electron microscopy (SEM) and thermal analysis techniques (TGA/DTG).

XRD results showed that clinoptilolite sample consisted of primarily clinoptilolite (80%). The impurities included volcanic glass (10%) and clay + quartz + biotite (10%). The chemical composition of clinoptilolite determined by X-ray fluorescence (XRF) measurements was as follows: SiO_2, 74.7%; Al_2O_3, 13.7%; Fe_2O_3, 1.45%; TiO_2, 0.15%; CaO, 2.76%; MgO, 0.69%; Na_2O, 1.07%; K_2O, 5.25%.

BET surface area was 54 $m^2\,g^{-1}$ and the total ion exchange capacity of Gördes clinoptilolite was approximately 2.8 meq/g, calculated as the sum of Mg, Ca, K and Na cations. This value was well consistent with those found for other two clinoptilolite samples around Aegean Sea, a Greek clinoptilolite of 2.62 meq/g and a Bigadic clinoptilolite of Turkey of 2.57 meq/g [8,9,11].

The actual metal oxide contents in the catalysts were measured using Thermo Elemental X Series ICP-MS and Varian Spectra Fast Sequential-220 atomic absorption spectrometer with an air-acetylene flame. Actual metal oxide loadings were listed in Table 1.

Surface areas of the catalysts after calcining at 500 °C for 4 h were measured by a Costech sorptometer 1042 equipment. Surface areas were obtained after further drying the samples in situ at 200 °C for 4 h to remove any moisture contamination in between calcination and BET measurement.

The morphology of powder catalysts was determined by Scanning Electron Microscopy (JEOL-5600 SEM −30 kV electron beam).

X-ray diffractions of powder samples were obtained on a Rigaku D/Max-2200 diffractometer by using the Cu Kα ($\lambda = 1.5405$) radiation. Samples were scanned from 10 to 80 at a rate of 0.5°/min (in 2Θ). The sizes of the crystalline domains were calculated by using Scherer equation, $t = C\lambda/B\cos\Theta$, where λ is the X-ray wavelength (A°), B is the full width at half maximum, Θ is Bragg angle, C is a factor depending on crystallite shape (taken to be one), and t is the crystallite size (A°). Relative crystallinity was calculated on the basis of comparing the average intensities for most intense peaks for the parent vs. treated zeolite catalyst.

Thermogravimetric analysis was performed using a Shimadzu TGA-60WS analyzer. All the samples were heated from 30 to 1000 °C with a heating rate of 10 °C/min using approximately 15 mg of sample powder under flowing air (50 ml/min). The decomposition behavior and weight loss steps were observed in TG/DTG curves.

Temperature-programmed reduction was performed to monitor the reduction of the metal oxide, from 60 to 600 °C. TPR profiles were measured by using Quantachrome ChemBET 3000 flow type equipment. In TPR experiments, 60 mg of the catalyst was dried at 105 °C for 2 h, and 10% H_2/N_2 (BOS, 99.99% purity) was used as a reducing gas. Temperature ramp rate was 10 °C/min and flow rate was 70 ml/min. The changes in H_2 flow were followed using a thermal conductivity detector.

Temperature-programmed oxidation profile was obtained by using Quantachrome ChemBET 3000 flow type equipment. After TPR experiments, the reduced sample are oxidized using air with a flow rate of 70 ml/min, increasing the temperature from room temperature to 600 °C at a heating rate of 10 °C/min. After reaching 600 °C, the temperature is cooled down to room temperature on its own.

Temperature-programmed desorption of ammonia was performed on a Quantachrome ChemBET 3000 instrument in order to evaluate the acidic properties of the oxides. Prior to adsorption experiments, samples (60 mg) were first pre-treated in a quartz U-tube in a N_2 stream at 500 °C, and subsequently cooled down at 100 °C in an He flow (20 $cm^3\,min^{-1}$). The adsorption step was performed by admitting small pulses of ammonia in He at 100 °C up to saturation. Subsequently, samples were exposed to a flow of helium (50 $cm^3\,min^{-1}$) for 2 h at 100 °C to remove reversibly and physically bound ammonia from the surface. Finally, desorption was carried out from 100 to 550 °C at a heating rate of 10 °C min^{-1} in helium stream (50 $cm^3\,min^{-1}$). Flowing helium largely inhibited the eventual readsorption of NH_3. The desorbed ammonia was detected by a thermal conductivity detector, and quantified by time integration of areas under desorption curves.

The acidic properties of catalysts were also investigated by *n*-butyl amine desorption using a Shimadzu TGA-60WS thermogravimetric analyzer.

2.2. Preparation of zeolite used as support

The natural clinoptilolite was converted to homoionic sodium form prior to metal oxide loading experiments in order to increase its exchange capacity. For this purpose, clinoptilolite samples were treated with 0.1 M NaCl solution prepared using a Merck reagent-grade salt in deionised water at 30 °C in a shaking water bath for 2 h. Solid phases were separated by centrifuging at 4000 rpm. Sodium exchanged clinoptilolite sample was washed with deionized water several times until all traces of Cl^- anions were removed and verified the absence of chlorine residues with $AgNO_3$ and dried in oven at 110 °C.

2.3. Catalyst preparation

Two different zeolitic materials, clinoptilolite and, for comparison purposes, NH_4ZSM-5 ($SiO_2/Al_2O_3 = 30$, BET surface area of 400 $m^2\,g^{-1}$) available in the interval 40/60 mesh were studied and compared. NH_4ZSM-5 was prepared by treating ZSM-5 samples as received and treated with 0.1 M NH_4Cl solution prepared using a Merck reagent-grade salt in deionised water at 30 °C in a shaking water bath for 2 h. NH_4ZSM-5 was simply used after calcination at 500 °C for 4 h and it was believed that NH_4ZSM-5 was converted in HZSM-5 form.

Transition metal solutions (0.25 M) were prepared by dissolving $Co(NO_3)_2{\cdot}6H_2O$ (Merck), $Fe(NO_3)_3{\cdot}9H_2O$ (Merck) and of $Mn(NO_3)_2{\cdot}4H_2O$ (Merck) in distilled water. Ion exchange between zeolites and Co(II), Fe(III) or Mn(II) solutions was allowed to take place by adding zeolite into the metal solution. The transition metal salt loaded zeolites were recovered by filtration and repeatedly washed with distillate water to remove the nitrates completely. The filtrated paste was dried at 105 °C for 14 h, and then calcination was carried out at 500 °C in an oven under flowing air for 4 h. The resultant powder was ground at a constant vibration rate of 300 rpm for 15 min in a Retsch MM 200 vibrant-ball mill by using ZrO_2 milling container with 12 mm ZrO_2 milling balls. Particulate size was determined to be as 53–90 μm. Metal oxide loading of the catalysts was nominally 3, 5 and 9.5 wt% and reported as weight percentages of their common oxides, Co_2O_3, Fe_2O_3, and MnO_2. For instance, 9.5MnO_2/NaCLT means that the catalyst contained nominally 9.5% MnO_2 by weight and deposited on to NaCLT support.

2.4. Catalytic activity

Catalytic activity was determined using a fixed-bed reactor, in which typically 0.15 g of catalyst was loaded between glass wool packing. Reactor was build of stainless steel with an internal diameter of 4 mm, which was one pass flow through reactor. Empty reactor was tested for any kind of activity at the harshest conditions and there were no activity of the reactor itself. Prior to catalytic tests, catalyst precursors were activated by heating in flowing air up to 500 °C at the rate of 10 °C/min, and annealed at this temperature for 1 h. Catalytic activity of the calcined samples was measured in total combustion of toluene in air. The reaction feed consisted of 1000 ppm of toluene balance being dry air. The feed stream was prepared by delivering toluene by a syringe pump (Cole Palmer 74900-05) into dry air, which was metered by a mass flow controller (Brooks, 5850TR). A total flow rate of 500 $cm^3\ min^{-1}$ was used and catalysts were packed to a constant volume to give a gas hourly space velocity of 15,000 h^{-1} for all studies. Catalytic activity was measured over the range of 150–550 °C, and operating temperatures were measured by a thermocouple placed in the catalyst bed. Conversion data were calculated by the difference between inlet and outlet concentrations. Conversion measurements and product profiles were taken at steady state, typically after 30 min on stream. On some selected low activity catalysts, we have carried out repeat experiments to determine the scattering and it was found that experiments were highly repeatable since we have utilized an internal standard in the inlet gas composition. This method of analysis resulted in high degree of accuracy and repeatability too. The feed and the reaction products were analyzed by on-line gas chromatograph (HP 6890+) equipped with a thermal conductivity detector (TCD) and a flame ionization detector (FID) in series. The hydrocarbons and carbon dioxide were analyzed with a Poraplot Q capillary column (30 m × 0.530 mm × 40 μm) and carbon monoxide with a Molecular Sieve 5A capillary column (30 m × 0.530 mm × 50 μm), both columns being connected in parallel.

3. Results and discussion

BET surface areas of supported metal oxide catalysts were measured and found to be as follows: 9.5MnO_2/NaCLT (32 $m^2\ g^{-1}$) > 9.5Co_3O_4/NaCLT (26 $m^2\ g^{-1}$) > 9.5Fe_2O_3/NaCLT (21 $m^2\ g^{-1}$). Surface areas of the supported Mn, Co and Fe oxides' catalysts were found to have decreased 40, 52 and 61% in comparison to that of pristine support's surface area, respectively. Since the changes in surface areas were not as drastic as the changes in catalytic activities, hence the activity patterns were likely due to the active species on the surface.

Images obtained by using SEM allow us to see the support structure. Fig. 1a–d presented SEM images of natural and metal oxide loaded clinoptilolites, which indicated the presence of crystals with some crystal faces with various particle sizes. In the present paper, the SEM pictures of some clinoptilolite (Fig. 1a) samples are well correlated with the literature data. As follows from Fig. 1b–d after ion exchange processes, basic processing the clinoptilolite surface did not change it noticeably, which can be explained by the fact that elution of exchange cations occurred but it did not result in the elution of silicium or aluminium of the zeolitic backbone. In addition, as a result of ion exchange processes, recrystallization in alkaline medium did not occur and this was visible from the SEM pictures since no marked change was observed on the SEM pictures.

3.1. X-ray powder diffraction

Clinoptilolite was the major crystalline phase detected on the X-ray diffraction pattern as shown in Fig. 2a. XRD peaks of clinoptilolite sample were found to be in good agreement with the data of clinoptilolite, JCPDS card (83-1260). In addition to zeolitic phase, quartz, cristobalite, and K-feldspar in minor quantities were also detectable in X-ray diffraction patterns. The clinoptilolite content of the sample was estimated to be higher than 80% (w/w).

The diffraction patterns, shown in Fig. 2b, were of three different metal oxides phases. XRD patterns well matched with the diffraction patterns of crystalline orthorhombic Fe_2O_3 (JCPS 52-1449), cubic Co_3O_4 (JCPS 42-1467) and tetragonal MnO_2 (JCPS 44-0141). The reflections present in the XRD of the various metal oxides/NaCLT samples belonged to the most intense lines. Fig. 2c shows the effect of increasing metal oxides content. As the manganese oxide content increased, MnO_2 peaks became more apparent whereas for 3% Mn loaded sample MnO_2 phases were not distinctly apparent. Crystallinity percentage and crystallite sizes of oxide phase in samples were also calculated and listed in Table 1. It was observed that metal oxide crystallite size, % crystallinity and weight loss increased as metal oxide content increased as expected.

3.2. Temperature-programmed reduction (TPR) and oxidation (TPO)

The reducibility of Mn sites in clinoptilolite was studied by H_2-TPR. These measurements were carried out on transition metal exchanged and calcined catalysts, and allowed us to estimate the reducibility of metal oxide species, which depended on the interactions with exchanged zeolites framework. Exemplary TPR profiles of used and fresh catalysts were depicted in Fig. 3a.

9.5MnO_2/NaCLT catalyst showed two reduction peaks at 362 and 468 °C in TPR profile, whereas used 9.5MnO_2/NaCLT catalyst showed no peaks at all. This result clearly demonstrated that the catalyst was quantitatively reduced after reaction temperature reached at 500 °C. TPR profiles showed the first step of reduction ended at around 397 °C. It is worthwhile to note that 9.5MnO_2/NaCLT catalyst started to lose its maximum activity after reaching 350 °C. Temperature at which first step of reduction presented a maximum at 362 °C (see Fig. 3a) was well in agreement with 350 °C at which 9.5MnO_2/NaCLT showed maximum activity. Remaining activity at around 20% toluene conversion at temperatures beyond 350 °C was considered to be probably due to the sites still in their oxidized states of those possibly having higher interaction with zeolite frame. TPR profiles showed the second reduction peak maximum at 468 °C. TPR patterns were used to assess the degree of interaction between the exchanged ion and the zeolite

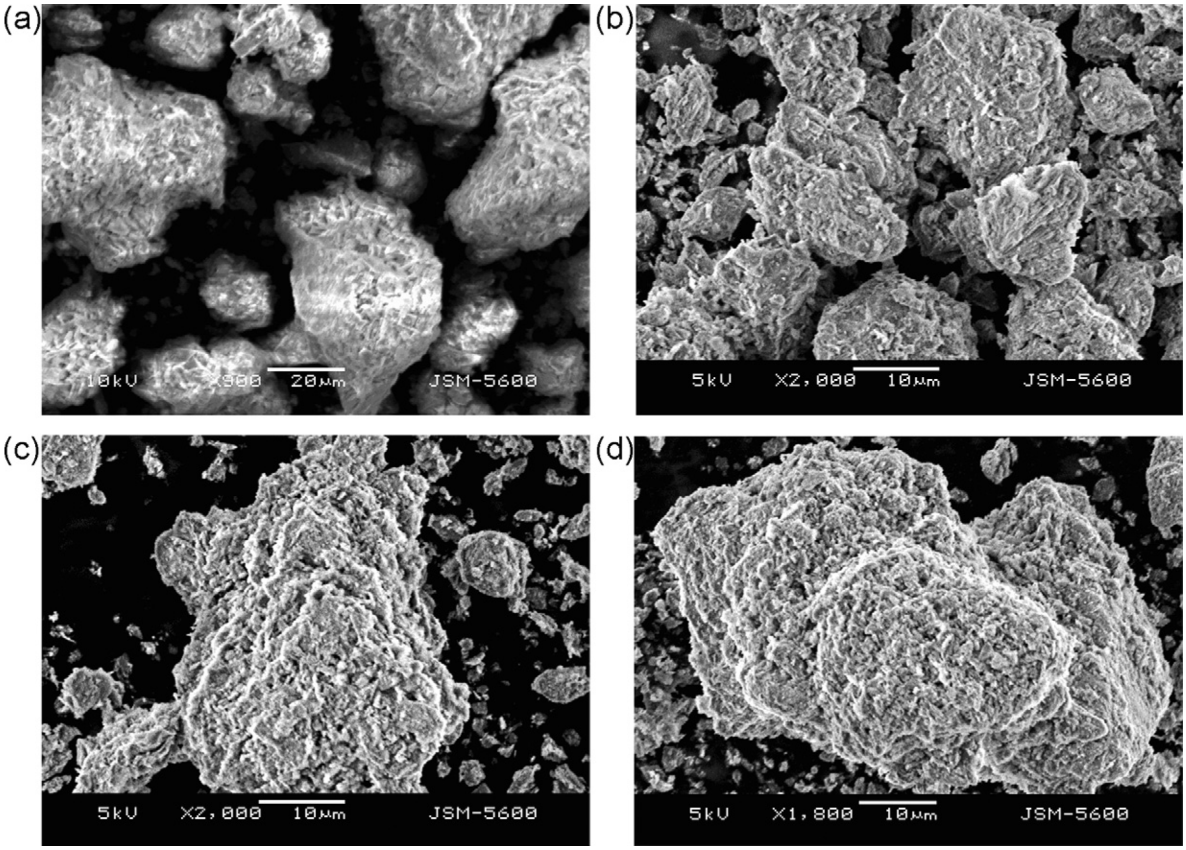

Fig. 1. SEM images of (a) NaCLT, (b) 9.5MnO_2/NaCLT, (c) 9.5Co_3O_4/NaCLT, and (d) 9.5Fe_2O_3/NaCLT catalysts.

framework. Actually, the redox properties of the Mn were strongly affected by the zeolite support. At this point, Goursot et al. [14] state that the zeolite framework acts as a reservoir of charge for the redox reactions of the transition metal ion. These results suggested that the cations were not located in the zeolite structure but rather on the surface. In literature, it was observed that the iron (or at least an important fraction of it) presents only slight interaction with the zeolite framework [15].

Used catalyst was subjected to a temperature-programmed oxidation treatment, and the catalyst was reoxidised in two steps approximately at around temperatures where reduction steps were observed. It was also observed that during oxidation, reoxidised surface areas were much smaller than reducible surfaces. This led us to the conclusion that at least some portion of reduction was followed by some surface area lost.

The reoxidation of Mn sites in clinoptilolite was studied by O_2-TPO. The result from TPO experiment is depicted in Fig. 3b. TPO profile of 9.5MnO_2/NaCLT catalyst shows two peaks at 264 and 340 °C representing oxygen consumption during the reoxidation process. TPO profile showed the second step of reoxidation ended at around 480 °C. The result shows that the reoxidation of metallic Mn to MnO_2 can proceed. However, the oxygen consumption temperatures decrease and also shift to lower temperature after reduction process.

3.3. *Acidity measurements*

Amine adsorption method on acid sites of solid catalysts is a well-known technique to determine the acidity of the catalyst. The use of *n*-butyl amine as molecular probe for the characterization of catalysts has been reported [16–18] and used in this study too.

Differential thermogravimetric (DTG) desorption curves of *n*-butyl amine were obtained for various catalysts. Based on weight loss values of *n*-butyl amine treated catalysts, amount of adsorbed *n*-butyl amine was calculated quantitatively. As shown in Table 2, catalysts had three desorption steps depending on their acidity. These were the desorption peaks of physisorbed *n*-butyl amine before 117 °C, of *n*-butyl amine from medium acid sites of the catalysts indicated by the second peak in DTG curves at about 300 °C. Desorption of the *n*-butyl amine from strong acid sites of the catalysts indicated by the third group of peaks observed at 483–979 °C. 9.5MnO_2/NaCLT had the highest peak intensity in medium acid sites. All other catalysts had weak, medium and strong acidity to a lesser extent. As shown in Table 2, medium strength acidity was found to decrease in following order: MnO_2/NaCLT > Co_3O_4/NaCLT > Fe_2O_3/NaCLT.

To verify and consolidate the *n*-butyl amine findings, NH_3-TPD profile of 9.5MnO_2/NaCLT was taken and shown in Fig. 4, revealing the presence of acid sites with varying strengths on calcined 9.5MnO_2/NaCLT. The temperature range in which the ammonia desorbed was an indicator of the strength of the acid sites. An attempt to characterize the strength of acid sites was made by integrating two peaks observed in the TPD profiles. The desorption peaks were invariably located at around 250 and 385 °C. The peaks at 250 °C and below were related to the weak acidity present in the catalysts, while the higher temperature peaks (385 °C) were assigned to the sum of medium and strong acidity. These results were confirmed and found to be in line with the data obtained from the amine adsorption method. In conclusion, the most acidic catalyst was found to be 9.5MnO_2/NaCLT.

3.4. *Catalytic tests*

Calcination of catalysts at high temperatures might lead to the sintering of active species on the surface and reaction between catalytically active species and residual species on zeolite. Hence,

Table 2
Density of zeolite acid sites, ΔT = temperature range between *n*-butyl amine (NBA) desorbed, δ, is calculated and δ = acidity in mmol NBA/g_{cat}.

Catalysts (metal oxide/zeolite)	Weak sites		Medium + strong sites		δ_{total} (mmol/g_{cat})
	ΔT (°C)	δ (mmol/g_{cat})	ΔT (°C)	δ (mmol/g_{cat})	
$3MnO_2$/NaCLT	111–250	0.443	250–807	0.295	0.738
$5MnO_2$/NaCLT	75–225	0.562	225–832	0.493	1.055
$9.5MnO_2$/NaCLT	70–202	0.583	202–868	0.702	1.285
$9.5MnO_2$/HZSM-5	33–269	0.761	210–718	1.115	1.876
$9.5Co_3O_4$/NaCLT	78–226	0.565	208–802	0.581	1.146
$9.5Fe_2O_3$/NaCLT	71–208	0.460	226–810	0.427	0.887

the effect of calcination temperature on the conversion of toluene during light-off experiments was investigated and shown in Fig. 5. It was seen that toluene conversion decreased from 94 to 28% with an increase of calcination temperature from 500 to 700 °C. This result showed calcination at higher temperatures resulted in the loss of active species on the catalyst surface, probably through sintering and increased interaction of metal oxide species with the content of zeolite framework. Li et al. also observed that an increase in calcination temperature from 300 to 800 °C induced a decrease in the catalytic activity from 87.1 to 0% [19].

The oxidation activity was recorded by following the evolution of conversion with temperature (the so-called light-off curves). The selectivity towards CO_2 was almost 100% and no intermediates, such as CO or other hydrocarbons, were detected. The decomposition of toluene started above 150 °C, reaching the maximum oxidation near 350 °C for all the catalysts studied. Then, above 350 °C, the activity decreased sharply and leveled out at around 20%. Fig. 6 showed the catalytic conversions attained as a function of temperature over $9.5MnO_2$/NaCLT, $9.5Co_3O_4$/NaCLT, $9.5Fe_2O_3$/NaCLT and $9.5MnO_2$/HZSM-5. For $9.5MnO_2$/NaCLT, $9.5Co_3O_4$/NaCLT, $9.5Fe_2O_3$/NaCLT, the maximum CO_2 conversion was 93.02, 32.08 and 16.90%, respectively, at a reaction temperature of 350 °C. $9.5MnO_2$/HZSM-5 catalyst showed a maximum activity at around 400 °C, and $9.5MnO_2$/HZSM-5 catalyst did not show any activity peak as such the catalysts on NaCLT support did. Values of ignition temperature or T_{50} were reported in Table 2.

For comparison, these experiments were also carried out over $9.5MnO_2$ loaded on commercial HZSM-5 catalyst, T_{50} and T_{90} values were not obtained under the conditions studied here. Toluene conversion reached 24.78% at 350 °C. It was clearly seen that the CO_2 yield was higher over $9.5MnO_2$/NaCLT catalyst. However, such a peculiar reduction of activity after reaching maximum at intermediate temperature was not observed over ZSM-5 support. This finding led to the conclusion that remnants of calcination or support surfaces itself effected negatively surface active MnO_2 species above 350 °C.

To determine optimum calcination temperature, the dried samples were characterized by TGA/DTG under flowing air. From a typical TGA curve, thermogravimetric analysis of ($9.5MnO_2$/NaCLT) catalyst after being metal exchanged showed the weight loss in one distinct region between 100 and 700 °C, which corresponded to total 16.11% weight loss. The weight loss was primarily ascribed to the decomposition of carbonaceous and nitrate species remnant of precursor materials. Major weight loss ended below 500 °C, therefore, calcination at 500 °C under flowing air was considered to be sufficient to obtain corresponding metal oxides. Since all the metals utilized as precursor was in nitrate forms with some crystalline water, all the catalysts were shown similar thermogravimetric behavior. Hence, 500 °C was adopted as calcination temperature for the rest of catalysts.

Morphology of 9.5Mn/NaCLT, 9.5Co/NaCLT and 9.5Fe/NaCLT catalysts were shown in Fig. 1a–c, respectively. The particles were almost regular in shape. It was also observed that after metal exchange process, the particles kept original shape and were rather homogeneous in terms of size uniformity.

Among the catalysts utilized, namely, $9.5MnO_2$/NaCLT, $9.5Co_3O_4$/NaCLT, $9.5Fe_2O_3$/NaCLT, $9.5MnO_2$/NaCLT catalyst showed most peculiar behavior hence, it was chosen for further studies. Support, clinoptilolite, also contained some minor quantities of reactive metal oxides, such as Na_2O, CaO. Thus, this very low activity even at temperatures above 350 °C can be due to interaction between active species and these metal oxides present in the framework of zeolite. Due to the interaction (of unknown type) between the exchanged ion (Na^+) and the species on zeolite, increasing temperature from 350 °C resulted in the decrease in catalytic activity for all three Fe, Co and Mn catalysts. This negative effect could be tentatively explained in two ways. First explanation was that the catalysts were reduced to their corresponding metallic states irreversibly this reduction was made easy by the presence of oxides within the framework of zeolite and second tentative explanation was that higher temperatures (350 °C) suppressed the sorption of toluene. There was experimental evidence which supported the first explanation from TPR experimentation as shown in Fig. 3. Because of the method utilized in this study (short ion exchange times, i.e., 2 h), complete removal of surface active species coming from natural zeolite were not achieved, therefore, at temperatures above 350 °C, MnO_2 (and other metal oxides too) species were subjected to complete reduction made easy by the presence of oxides present within the framework and therefore, led to reduced activity.

The performance of MnO_2/NaCLT catalysts in the toluene combustion was also studied at various MnO_2 loadings. Fig. 7 showed the influence of MnO_2 loading on the toluene combustion as a function of reaction temperatures. In all three cases of loadings, the only reaction products were only carbon dioxide and water.

The CO_2 percentages increased with increasing MnO_2 content up to 9.5%, above which all values remained relatively constant being reached at maximum conversion. The 93.02% CO_2 conversion was obtained at 350 °C. The order of activity increased with an increase in MnO_2 content as follows: $3MnO_2$/NaCLT < $5MnO_2$/NaCLT < $9.5MnO_2$/NaCLT. This finding also proved that the increase of activity was actually caused by increasing Mn content and hence leading to the conclusion of that the activity was provided by the sites of MnO_2. The increased activity was also followed by the increase in weak acid sites as listed in Table 2. Moreover, there was similar pronounced relationship between medium + strong acid sites and catalytic activity (Table 2). The highest acid site concentration observed was over $9.5MnO_2$/NaCLT catalyst.

The results were shown in Table 2 where combustion temperature was referred to the temperature the toluene conversion reached maximum. It was clearly observed that combustion temperature ranges were very similar with that for the metal oxides/NaCLT catalysts except for 9.5Mn/HZSM-5, MnO_2 and NaCLT. It was experimentally found that addition of metal oxide into clinoptilolite led a decrease in combustion temperature and an increase in toluene conversion, in general. It was noteworthy to remind that MnO_2 alone showed a higher combustion peak temperature than $9.5MnO_2$/NaCLT. As a result, using of metal sites in the structure of metal impregnated and zeolite supported catalyst in

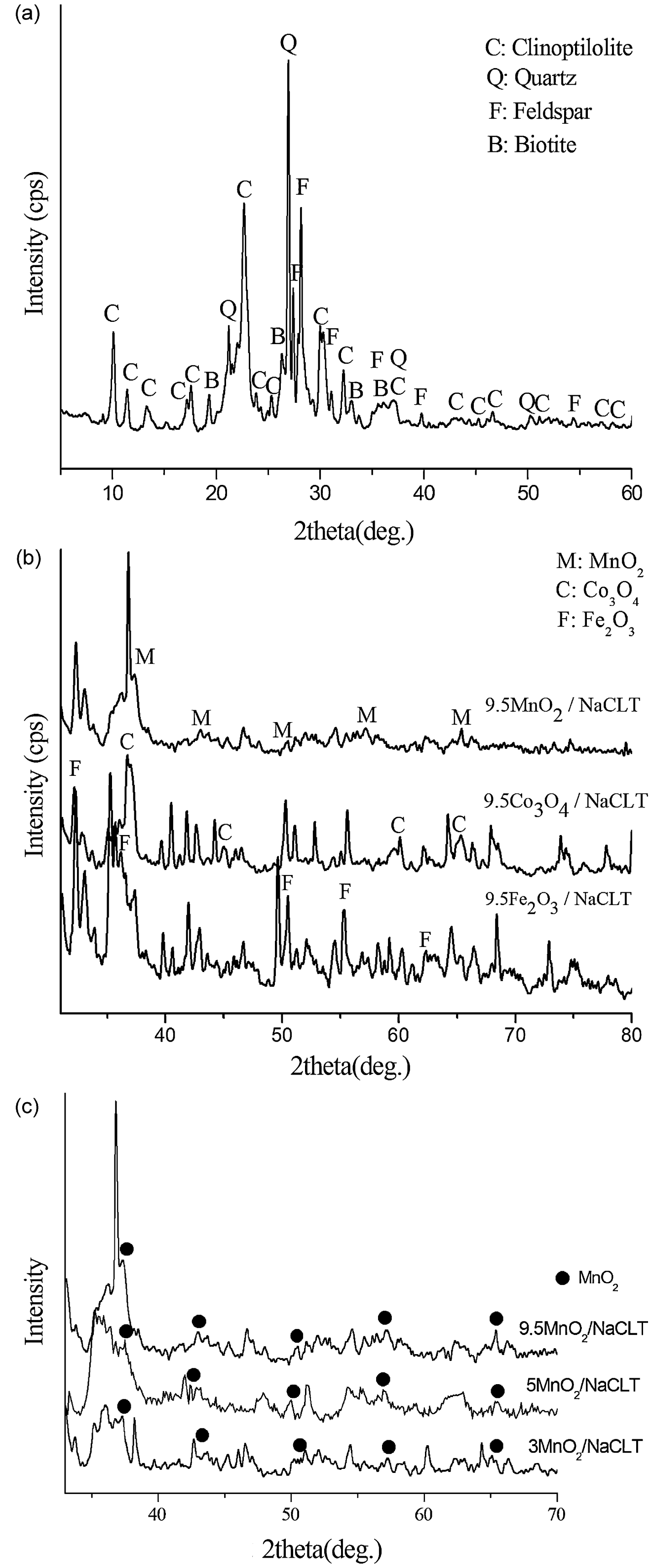

Fig. 2. (a) XRD patterns of NaCLT. (b) XRD patterns of $9.5MnO_2$/NaCLT, $9.5Co_3O_4$/NaCLT, and $9.5Fe_2O_3$/NaCLT catalysts. (c) XRD patterns of MnO_2/NaCLT catalysts of various compositions.

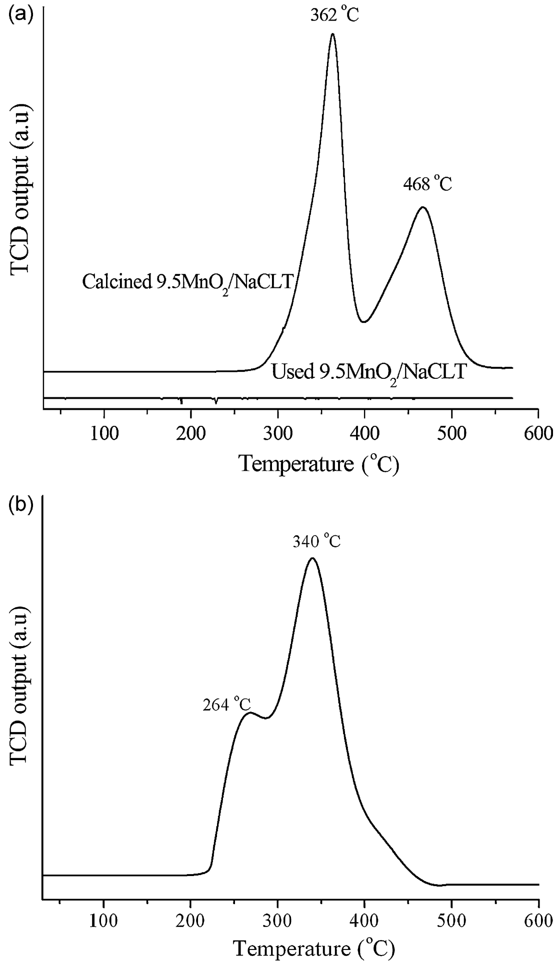

Fig. 3. (a) TPR profiles of the catalysts. (b) TPO profile of $9.5MnO_2$/NaCLT catalyst.

the oxidation process, it is understood that the metal impregnated catalyst could improve oxygen adsorption property. This may be due to the strong interaction between manganese and NaCLT as well as the well-known high temperature stable property of CLT. Hence, support zeolite facilitated the combustion and also the lowered the on-set of combustion too. It is also worthy to say that species remaining on the surface of zeolite also obstructed and irreversibly detoriated the activity beyond 350 °C.

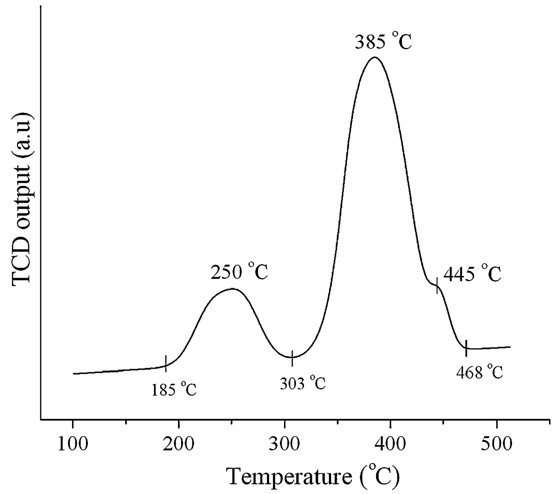

Fig. 4. Ammonia TPD profile of calcined $9.5MnO_2$/NaCLT.

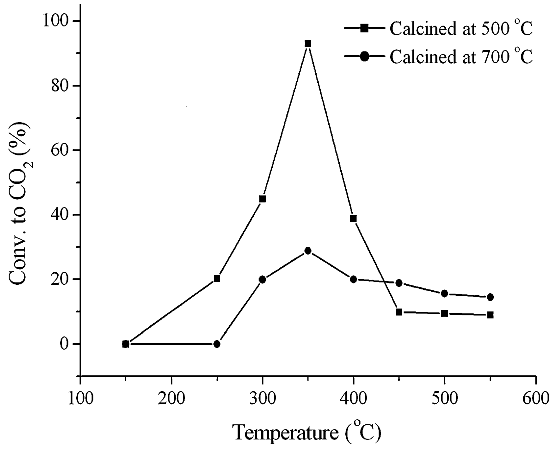

Fig. 5. Toluene conversion vs. reaction temperature over 9.5MnO_2/NaCLT catalyst calcined at various temperatures.

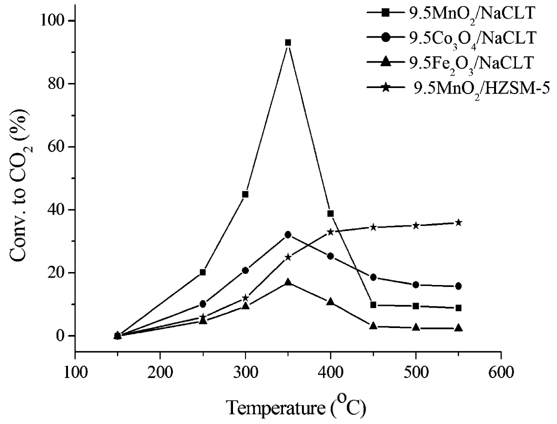

Fig. 6. Light-off curves of combustion of toluene vs. reaction temperature over different catalysts.

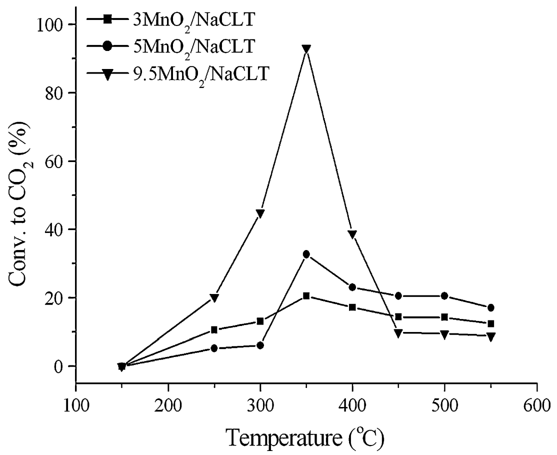

Fig. 7. Toluene conversion vs. reaction temperature with various MnO_2/NaCLT catalysts.

4. Conclusion

The toluene combustion was studied over catalysts containing Co, Fe and Mn common oxides. Increase in activity was paralleled by increasing metal oxide content for all three catalyst types up to 9.5% by weight.

It has been found that manganese oxide exhibited higher catalytic activity for the low-temperature catalytic combustion of toluene than other two oxides. 9.5MnO_2/NaCLT catalyst showed the catalytic conversion of toluene to 93% at a temperature of 350 °C. However, due to the interaction between the exchanged ion and the zeolite, increasing combustion temperature above 350 °C led to major decrease in activity. Addition of metal oxide into clinoptilolite resulted in a decrease in combustion temperature and an increase in toluene conversion.

Characterization and reactivity data indicated that the reactivity of toluene was determined by the strength of the surface acidity. NaCLT type zeolite facilitated the combustion and also lowered the on-set of combustion, too. Manganese oxides impregnated NaCLT support showed unusual features too. 9.5MnO_2/NaCLT combination is worthy for further detailed study.

Acknowledgements

This work was supported by TUBITAK-ÇAYDAG for the financial support within the research project 107Y096 [2007–2009].

References

[1] A. Musialik-Piotrowska, Destruction of trichloroethylene (TCE) and trichloromethane (TCM) in the presence of selected VOCs over Pt–Pd-based catalyst, Catal. Today 119 (2007) 301–304.
[2] Council Directive 1999/13/EC, The limitation of emissions of volatile organic compounds due to the use of organic solvents in certain activities and installations, Off. J. Eur. Commun. (1999) 1–22.
[3] F.I. Khan, A.Kr. Ghoshal, Removal of volatile organic compounds from polluted air, J. Loss Prevent. Process Ind. 13 (2000) 527–545.
[4] J.J. Spivey, Complete catalytic oxidation of volatile organics, Ind. Eng. Chem. Res. 26 (1987) 2165–2180.
[5] J. Carpentier, J.F. Lamonier, S. Siffert, et al., Characterisation of Mg/Al hydrotalcite with interlayer palladium complex for catalytic oxidation of toluene, Appl. Catal. A: Gen. 234 (2002) 91–101.
[6] T. Takeguchi, S. Aoyama, J. Ueda, R. Kikuchi, K. Eguchi, Catalytic combustion of volatile organic compounds on supported precious metal catalysts, Top. Catal. 23 (1–4) (2003) 159–162.
[7] Y. Liu, M.F. Luo, Z.B. Wei, Q. Xin, P.L. Ying, C. Li, Catalytic oxidation of chlorobenzene on supported manganese oxide catalysts, Appl. Catal. B: Environ. 29 (1) (2001) 61–67.
[8] M. Ferrandon, E. Bjornbom, Hydrothermal stabilization by lanthanum of mixed metal oxides and noble metal catalysts for volatile organic compound removal, J. Catal. 200 (1) (2001) 148–159.
[9] M.C. Alvarez-Galvan, V.A.D.P. O'Shea, J.L.G. Fierro, P.L. Arias, Alumina-supported manganese- and manganese–palladium oxide catalysts for VOCs combustion, Catal. Commun. 4 (5) (2003) 223–228.
[10] H.G. Lintz, K. Wittstock, Catalytic combustion of solvent containing air on base metal catalysts, Catal. Today 29 (1996) 457–461.
[11] M. Daturi, G. Busca, G. Groppi, P. Forzatti, Preparation and characterisation of $SrTi_{1-x-y}Zr_xMn_yO_3$ solid solution powders in relation to their use in combustion catalysis, Appl. Catal. B: Environ. 12 (4) (1997) 325–337.
[12] I.R. Iznaga, V. Petranovskii, G.R. Fuentes, C. Mendoza, A.B. Aguilar, Exchange and reduction of Cu^{2+} ions in clinoptilolite, J. Colloid Interface Sci. 316 (2007) 877–886.
[13] A. Corma, M.T. Navarro, From micro to mesoporous molecular sieves: adapting composition and structure for catalysis, Stud. Surf. Sci. Catal. 142 (2002) 487–501.
[14] A. Goursot, B. Coq, F. Fajula, Toward a molecular description of heterogeneous catalysis: transition metal ions in zeolites, J. Catal. 216 (2003) 324–332.
[15] E. Díaz, S. Ordónez, A. Vega, J. Coca, Catalytic combustion of hexane over transition metal modified zeolites NaX and CaA, Appl. Catal. B: Environ. 56 (2005) 313–322.
[16] V.J. Fernandes, A.S. Araujo, G.J.T. Fernandes, Thermal analysis applied to solid catalysts acidity, activity and regeneration, J. Therm. Anal. Calorim. 56 (1999) 275–285.
[17] D.R. Milburn, K. Saito, R.A. Keogh, B.H. Davis, Sulfated zirconia: attempt to use *n*-butylamine to measure acidity, Appl. Catal. A: Gen. 215 (2001) 191–197.
[18] R. Bezman, Characterization of acidic zeolites by thermometric titration, J. Catal. 68 (1981) 242–244.
[19] W.B. Li, M. Zhuang, J.X. Wang, Catalytic combustion of toluene on Cu–Mn/MCM-41 catalysts: influence of calcination temperature and operating conditions on the catalytic activity, Catal. Today 137 (2008) 340–344.